ACS Medicinal Chemistry Letters

pubs.acs.org/acsmedchemlett

Letter

Development and Characterization of Fluorescent Probes for the G Protein-Coupled Receptor 35

Lai Wei,[†] Kaijing Xiang,[†] Hongjian Kang, Yancheng Yu, Hongjie Fan, Han Zhou, Tao Hou, Yonglin Ge, Jixia Wang, Zhimou Guo, Yang Chen, Yaopeng Zhao,* and Xinmiao Liang*

Cite This: *ACS Med. Chem. Lett.* 2023, 14, 411−416

Read Online

ACCESS | Metrics & More | Article Recommendations | Supporting Information

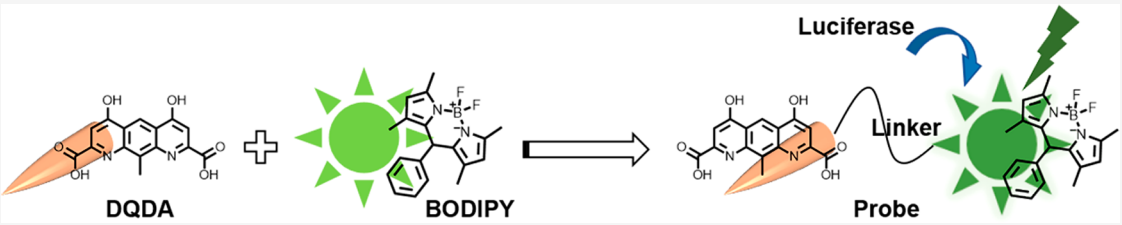

ABSTRACT: The orphan G protein-coupled receptor 35 (GPR35) is a potential target for the treatment of pain, inflammation, and metabolic diseases. Although many GPR35 agonists have been discovered, research on functional GPR35 ligands, such as fluorescent probes, is still limited. Herein, we developed a series of GPR35 fluorescent probes by conjugating a BODIPY fluorophore to **DQDA**, a known GPR35 agonist. All probes exhibited excellent GPR35 agonistic activity and desired spectroscopic properties, as determined by the DMR assay, bioluminescence resonance energy transfer (BRET)-based saturation, and kinetic binding experiments. Notably, compound **15** showed the highest binding potency and the weakest nonspecific BRET binding signal (K_d = 3.9 nM). A BRET-based competition binding assay with **15** was also established and used to determine the binding constants and kinetics of unlabeled GPR35 ligands.

KEYWORDS: *GPR35, fluorescent probes, bioluminescence resonance energy transfer, binding affinity*

GPR35 was first identified in 1998 and is believed to be associated with many diseases including coronary artery disease, cancers, and inflammatory bowel disease.[1−4] Although its endogenous activator remains controversial, a wide range of surrogate agonists are available.[5−8] However, there are few studies on functionalized GPR35 ligands, which are detrimental to the study of GPR35 physiological processes. Until now, 6-bromo-8-(4-[^{3}H]methoxybenzamido)-4-oxo-4*H*-chromene-2-carboxylic acid was the only molecule used in the GPR35 radioligand binding assays.[9]

BODIPY is considered a construction platform for fluorescent probes that are widely used in bioimaging and photodynamic therapy for their high molar absorption coefficients and fluorescence quantum yields as well as their good biocompatibility and photostability.[10,11] We previously reported a series of potent GPR35 agonists with two acidic groups located at each end of a fused tricyclic aromatic scaffold.[12] The structure−activity relationship (SAR) studies and docking simulations showed that the two terminal acidic groups were necessary for maintaining the high agonistic potency of the compounds, while substitutions in the middle of the scaffold were tolerated.[12] Considering the high potency of the compounds and the convenience of the synthesis, we chose4,6-dihydroxy-10-methylpyrido-[3,2-g]-quinoline-2,8-dicarboxylic acid (**DQDA**) as a molecular moiety to target GPR35 (EC_{50} = 8.0 nM).

10-(*p*-Alkoxyphenyl)-BODIPY was selected as the fluorophore to couple with the hydroxyl of **DQDA**, since its absorption band between 460 and 520 nm overlaps well with the emission band of NLuc, creating a possibility for BRET between the NLuc-tagged GPR35 and the fluorescent probes.

The syntheses of the GPR35 fluorescent ligands **14**−**17** are depicted in Figure 1. The dimethyl 4,6-dihydroxy-10-methylpyrido- [3,2-*g*]-quinoline-2,8-dicarboxylate (**1**) was prepared as previously described.[12] The iodoalkynes (**2**−**4**) reacted with compound **1** to produce intermediates **5**−**7**. Compound **1** could be converted into intermediate **8** through the introduction of the oxa-alkyne in the Mitsunobu reaction. Using a typical copper-catalyzed azide−alkyne cycloaddition, BODIPY containing an azide group (**9**) was conjugated with **5**−**8** to yield compounds **10**−**13**, respectively. These methyl

Received: October 25, 2022
Accepted: February 15, 2023
Published: February 22, 2023

https://doi.org/10.1021/acsmedchemlett.2c00461
ACS Med. Chem. Lett. 2023, 14, 411−416

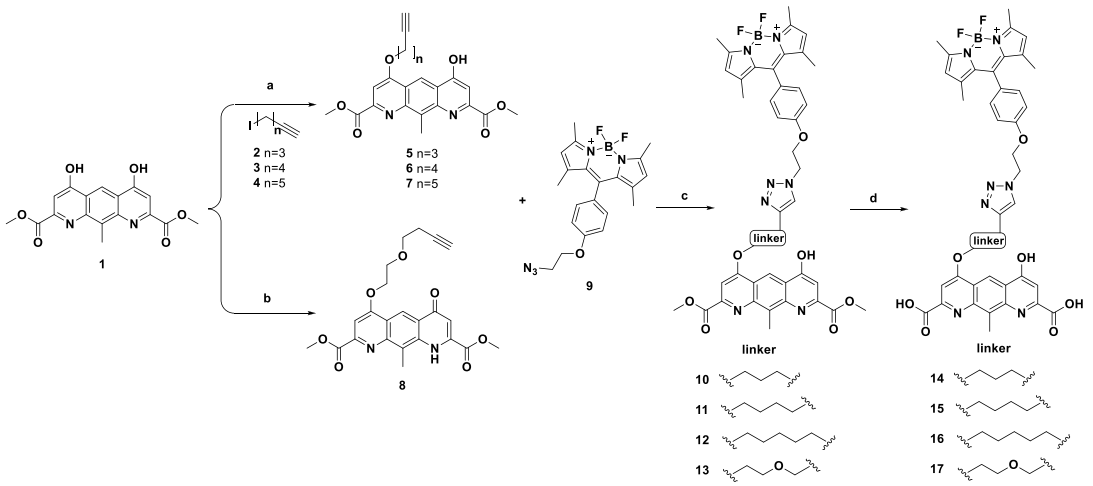

Figure 1. Syntheses of BODIPY-labeled fluorescent probes **14**−**17**. Reagents and conditions: (a) Cs_2CO_3, DMF, at 50 °C overnight, 34−47% (b) 2-(prop-2-yn-1-yloxy)ethan-1-ol, PPh_3, DIAD, THF, from 0 °C to room temperature overnight, 35%. (c) $CuSO_4{\cdot}5H_2O$, sodium ascorbate, THF: H_2O (1:1, v/v), at 50 °C overnight, 73−81%. (d) LiOH, H_2O: MeOH (1:1, v/v), at room temperature for 2 h, 65−81%.

ester products were hydrolyzed with lithium hydroxide to yield BODIPY-labeled fluorescent ligands **14**−**17**.

BODIPY derivatives with extended conjugated structures often exhibit a significant positive or negative solvatochromic effect in different polar environments.[13−15] Some simple derivatives of BODIPY are characterized by a small Stokes shift and a solvatochromic effect on the polarity of the medium.[16] We recorded the UV absorption and fluorescence spectra of probes **14**−**17** in PBS solution, a standard aqueous buffer used in *in vitro* pharmacological assays, and in *n*-octanol, an organic solvent usually used to mimic a predominantly hydrophobic environment like the receptor binding site or cell membrane (Figures S1 and S2). These fluorescent probes showed low solvatochromic behavior in the solvents, with both the absorption maxima and emission maxima showing little change (Table S1). In *n*-octanol, the probes displayed an absorption maximum at 502 nm and a fluorescence maximum at 512 nm with a 10 nm Stokes shift. These results were consistent with literature reports[16] and were expected since the BODIPY unit of the probe was simply tethered to the target head DQDA.

Using coumarin 153 as the reference, the relative quantum yields of all probes in *n*-octanol were determined and are listed in Table S1. Probe **15** exhibited the highest relative quantum yield (Φ) of 0.77. However, dramatic decreases in the absorption and fluorescence intensity were observed for all probes in PBS, with the emission maxima of **14**−**17** decreasing by 3- to 15-fold (Figure S1). The observed results can be reasonably attributed to the formation of an intramolecular charge transfer state that was stabilized by the polar environment to give lower Φ values.[17] Figure S3 shows the fluorescence of in intramolecular charge transfer state that was stabilized by the polar environment to give lower Φ values.[17] Figure S3 shows the fluorescence spectra of probe **15** in various solvents, including PBS, H_2O, DMSO, methanol, ethanol, THF, dioxane, toluene, and *n*-octanol, further demonstrating the significant difference in intensity between organic solvents and aqueous solutions. The results showed that the quantum yield of the probes was highly sensitive to the environment, and the high fluorescence activity was preserved in the nonaqueous environment. Therefore, the background fluorescence from unbound probes in aqueous media should not be an issue.

DMR assays were applied to profile compound activity on GPR35 endogenously expressed in the human colorectal adenocarcinoma cell line HT-29. Zaprinast was used as a full agonist and tool molecule in DMR activation and desensitization experiments.[18,19] All four probes not only gave rise to the concentration-dependent DMR signals in HT-29 but also desensitized the DMR responses induced by 1 μM zaprinast after 1 h of incubation (Table 1 and Figure 2). All probes

Table 1. Pharmacologic Properties of Probes 14−17

	hGPR35		
Compd	EC_{50}[a] (nM)	IC_{50}[b] (nM)	IC_{50}[c] (nM)
zaprinast	0.71 ± 0.12	—	—
14	80.8 ± 9.5	9.6 ± 0.7	1034.1 ± 95.6
15	49.5 ± 5.6	9.4 ± 2.4	542.2 ± 87.3
16	42.2 ± 3.3	5.6 ± 0.8	397.6 ± 65.2
17	58.8 ± 5.8	7.8 ± 1.4	768.7 ± 84.6

[a]EC_{50} to trigger DMR. [b]IC_{50} to desensitize cells against repeated stimulation of 1 μM zaprinast. [c]IC_{50} of a known GPR35 antagonist ML-145 to block the agonist-induced DMR. The data represent mean ± SD from two independent measurements, each with four replicates (n = 2).

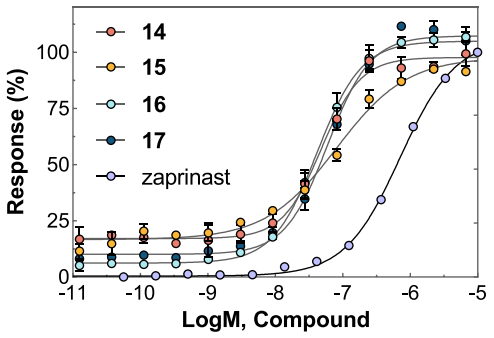

Figure 2. DMR response in HT-29 cells induced by fluorescent probes **14**−**17** as a function of the concentration. The data represent mean ± SD from two independent measurements, each with four replicates (n = 2).

https://doi.org/10.1021/acsmedchemlett.2c00461
ACS Med. Chem. Lett. 2023, 14, 411−416

exhibited high agonistic potency, with EC_{50} values between 42.2 and 80.8 nM. The GPR35 inhibitor ML-145 dose-dependently blocked the DMR responses generated by these probes (Table 1). Taken together, it is suggested that these probes generated DMR responses specifically through the activation of GPR35 in the HT-29 cells. To confirm this, these four ligands were further tested on two other cell lines. The CHO-K1 cell did not endogenously express GPR35, with none of the probes inducing the signals. However, in GPR35-overexpressing CHO-K1 cells, all the probes exhibited similar agonist activity and were confirmed to be GPR35 agonists (Figure S4).

A BRET-based GPR35 binding assay was then developed by using these fluorescent probes. It was performed as a homogeneous "mix and measure" assay well suited for kinetics and high-throughput equilibrium binding experiments.[20] CHO-K1 cells were transfected with hGPR35, which was N-terminally tagged with a nano-luciferase (NLUC).[21] NLUC has an emission maximum between 410 and 560 nm, displaying a partial overlap with the excitation spectra of probes, such as **15** (Figure 3). When the probe binds to

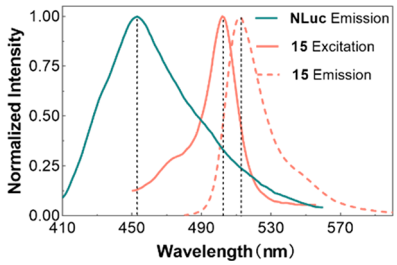

Figure 3. Emission spectrum of NLUC (dark green) and excitation (light red solid) and emission (light red dot) spectra of **15** were measured under the binding assay conditions.

NLUC-GPR35, energy transfer at 485 nm will occur between the NLUC and the BODIPY moiety, resulting in BODIPY emission at 528 nm. As BRET methods strictly depend on the distance between the bioluminescent and fluorescent partners, this approach would eliminate the need to remove the unbound probes from the assay medium.

Saturation binding experiments were performed by adding fluorescent probes at varying concentrations to the CHO-K1-hGPR35-NLUC cells. The results suggested that probes **14**–**17** could effectively respond to NLUC-tagged GPR35 via BRET (Figure 4). The nonspecific BRET signal was determined by coincubation with excess zaprinast (10 μM). Probes **14** and **16** displayed a considerable nonspecific BRET signal (Figure 4A and C), probe **15** showed a minor nonspecific BRET signal even at concentrations of up to 100 nM (Figure 4B), and probe **17** was in between (Figure 4D). The obvious difference was unexpected, as these probe linkers only differed slightly and may be related to the change of their fluorescence intensity in different polar environments. As shown in Figure S2, the fluorescence intensity of probe **15** in PBS decreased by a factor of 15 times that in *n*-octanol, changing more drastically than the other three probes. This difference might further reduce the signal of the nonspecific BRET signal shown in Figure 4B. The subtraction of the nonspecific BRET signal from the total binding signals generated monophasic binding curves with K_d = 7.4 ± 0.5 nM for **14**, K_d = 3.9 ± 2.5 nM for **15**, K_d = 8.3 ± 0.8 nM for

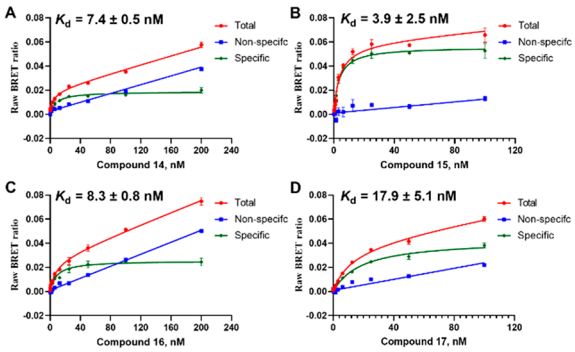

Figure 4. Saturation binding experiments of probes (A) **14**, (B) **15**, (C) **16**, and (D) **17** in CHO-K1-hGPR35-NLUC cells. Nonspecific bindings were measured by pretreatment with 10 μM zaprinast. The data represent mean ± SD from three independent measurements, each with three replicates (n = 3).

16, and K_d = 17.9 ± 5.1 nM for **17**. Among these potent candidates, probe **15** was selected for subsequent studies because of its high ratio of specific to nonspecific signals.

In the BRET kinetic binding experiments, the BRET emission ratio of **15** decreased drastically when GPR35 antagonist ML-145 was added, indicating a successful BRET between GPR35-NLUC and the probe molecule as a completely reversible binding process (Figure 6).

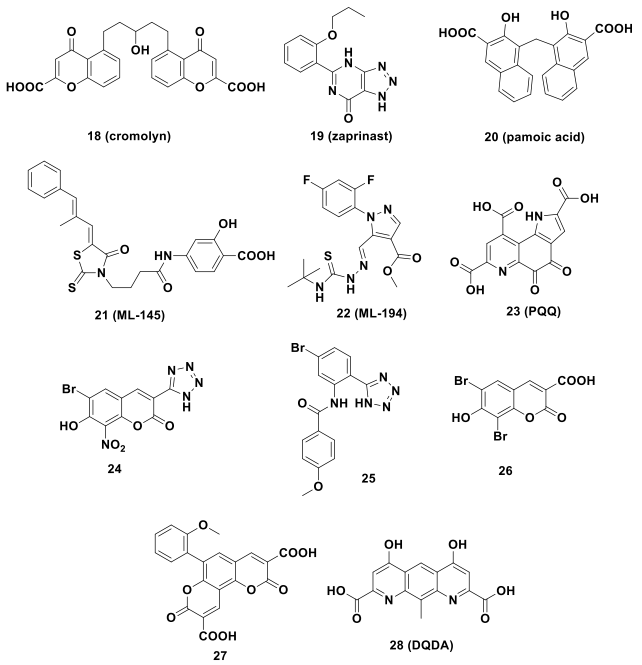

Figure 5. Structures of selected GPR35 ligands.

Next, we further investigated whether this BRET-based strategy using compound **15** as the probe could be applied to assess the affinity of GPR35 ligands, the structures are shown in Figure 5. The prerequisites for this application were that the binding of all of the active ligands was reversible and competed with probe **15** at the same GPR35 site. Competitive binding assays were conducted in CHO-K1 transferred with GPR35-NLUC by using **15** to assess the affinity of a range of previously reported GPR35 ligands (Figure S6). Some known GPR35 ligands were selected, such as agonists **18**–**20** and

https://doi.org/10.1021/acsmedchemlett.2c00461
ACS Med. Chem. Lett. 2023, 14, 411−416

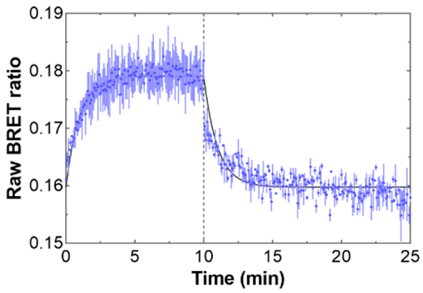

Figure 6. Kinetic binding experiment of probe **15**; 10 min after the addition of probe **15** (5 nM), ML-145 (10 μM) was added to dissociate the probe from GPR35.

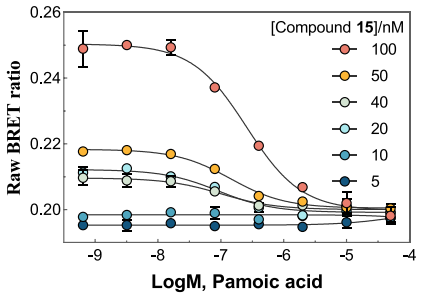

Figure 7. Application of **15** in competition binding experiments of pamoic acid **20**. Data represent mean ± SD from three independent measurements, each with three replicates (n = 3).

antagonists **21** and **22** (Figure 5). The results indicated that the selected molecules exhibited competitive binding against **15**, which allowed estimation of the K_i binding affinity constants. The K_i values measured by our BRET method were in agreement with those measured by the radioligand method reported in the literature (Table 2). These results indicated that this BRET-based binding assay should be a reliable strategy to measure the K_i values of the GPR35 ligands.

We further applied the BRET method to more GPR35 active ligands. Compounds **23**−**28** are the GPR35 agonists that we have previously discovered,[12,26,27] but their K_i values were not determined. Using the BRET method with compound **15** as a probe, these K_i values were measured for the first time and are listed in Table 2. Overall, a good correlation between agonist potency and binding K_i values was observed. Compound **28** the second most potent agonist in the functional assays displayed the highest binding affinity (Table 2). Likewise, **25**−**27** showed K_i values similar to those of their functional potencies. Unexpectedly, compound **24** was the most potent agonist in the DMR functional assays (EC_{50} = 0.006 μM) but showed a lower affinity in the BRET binding assay (K_i = 0.051 μM). Such a discrepancy between affinity and potency also existed in other similar studies and can be attributed to the different intrinsic efficacies of various compounds in the activation of GPR35.[27]

In addition, we evaluated whether the probe concentrations would affect the K_i values. Figure 7 shows the application of probe **15** in a competitive binding experiment with pamoic acid **20**. Higher concentrations of **15** required increasing concentrations of **20** to compete for the receptor binding site. However, the resulting K_i values of **20** varied in a narrow range (adding **15** at concentrations of 100, 50, 40, and 20 nM respectively provided K_i values of 9.6, 10.3, 8.9, and 14.9 nM) comparable to the K_i value of 12 nM reported previously (Table 2). It is worth noting that the BRET signals might be too low to be detected with the addition of probe **15** at 5 or 10 nM.

In conclusion, we describe the synthesis and evaluation of GPR35 fluorescent probes by tethering the BODIPY fluorophore to a known GPR35 agonist **DQDA**. The resulting probes **14**−**17** maintained excellent GPR35 agonistic activity with EC_{50} values between 42.2 and 80.8 nM. Probe **15** exhibits desirable spectroscopic properties, including good photostability, a Stokes shift of 10 nm, low fluorescence activity in aqueous solution, and a high quantum yield in nonpolar environments. In the NLuc construct built into the N-terminal domain of the GPR35 receptor and BRET-based binding experiments, probes **14**−**17** exhibited K_d values of 7.4, 3.9, 8.3, and 17.9 nM, respectively. Notably, probe **15** exhibited a favorable specific to nonspecific BRET signal at concentrations of up to 100 nM. The BRET-based binding assay with **15** was further applied to determine the kinetic binding parameters of unlabeled GPR35 ligands, resulting in K_i values comparable to those obtained previously using a radiolabeled ligand. This is the first report about the GPR35 fluorescent probe, demonstrating its utility for further study of the GPR35 receptor and ligand characterization.

Table 2. Potencies and Binding Affinities of the Selected GPR35 Ligands

Compd	BRET assay K_i (μM)[a]	Reference K_i (μM)[b]	DMR assay (μM)[c]	β-arrestin assay (μM)[d]
18	2.97 ± 0.87	2.340 ± 0.040	(EC_{50}) 0.52[22]	(EC_{50}) 7[22]
19	0.612 ± 0.233	0.401 ± 0.015	(EC_{50}) 0.16[23]	(EC_{50}) 4.2[23]
20	0.023 ± 0.006	0.012 ± 0.001	(EC_{50}) 0.003[24]	(EC_{50}) 1.20 ± 0.13[25]
21	0.004 ± 0.001	0.009 ± 0.001	/	(IC_{50}) 0.027[25]
22	0.236 ± 0.049	0.042 ± 0.003	(IC_{50}) 10.4[23]	(IC_{50}) 0.20[25]
23	0.332 ± 0.063	/	(EC_{50}) 0.071 ± 0.010[12]	/
24	0.051 ± 0.015	/	(EC_{50}) 0.006 ± 0.001[26]	(EC_{50}) 0.197 ± 0.038[23]
25	0.010 ± 0.002	/	(EC_{50}) 0.059 ± 0.007[28]	/
26	0.352 ± 0.107	/	(EC_{50}) 0.150 ± 0.020[26]	(EC_{50}) 3.63 ± 0.95[23]
27	0.028 ± 0.006	/	(EC_{50}) 0.083 ± 0.006[12]	/
28 (DQDA)	0.006 ± 0.002	/	(EC_{50}) 0.008 ± 0.001[12]	/

[a]Affinities were determined through displacement BRET binding assays using 25 nM **15**. The data represent mean ± SD from three independent measurements, each with three replicates (n = 3). [b]K_i values were acquired from radio−ligand binding assays from the literature.[9] /: not measured or reported. [c]EC_{50} values were tested by DMR assays in HT-29 cells endogenously expressing GPR35. [d]Previously published. /: not measured or reported.

https://doi.org/10.1021/acsmedchemlett.2c00461
ACS Med. Chem. Lett. 2023, 14, 411−416

■ ASSOCIATED CONTENT

Supporting Information

The Supporting Information is available free of charge at https://pubs.acs.org/doi/10.1021/acsmedchemlett.2c00461.

^{1}H NMR, ^{13}C NMR spectral data and HPLC-MS analysis of compounds **5**−**8** and **10**−**17**; molecular formula strings (PDF)

■ AUTHOR INFORMATION

Corresponding Authors

Yaopeng Zhao − *Key Lab of Separation Science for Analytical Chemistry, Dalian Institute of Chemical Physics, Chinese Academy of Sciences, Dalian 116034, China; Jiangxi Chinese Medicine Science Center of DICP, CAS, Nanchang 330000, China*; Phone: 86 411 84379519; Email: ypzhao@dicp.ac.cn

Xinmiao Liang − *Key Lab of Separation Science for Analytical Chemistry, Dalian Institute of Chemical Physics, Chinese Academy of Sciences, Dalian 116034, China; Jiangxi Chinese Medicine Science Center of DICP, CAS, Nanchang 330000, China*; orcid.org/0000-0003-4394-4274; Phone: 86 411 84379519; Email: liangxm@dicp.ac.cn

Authors

Lai Wei − *Key Lab of Separation Science for Analytical Chemistry, Dalian Institute of Chemical Physics, Chinese Academy of Sciences, Dalian 116034, China; Jiangxi Chinese Medicine Science Center of DICP, CAS, Nanchang 330000, China*

Kaijing Xiang − *Key Lab of Separation Science for Analytical Chemistry, Dalian Institute of Chemical Physics, Chinese Academy of Sciences, Dalian 116034, China; University of Chinese Academy of Sciences, Beijing 100049, China*

Hongjian Kang − *Key Lab of Separation Science for Analytical Chemistry, Dalian Institute of Chemical Physics, Chinese Academy of Sciences, Dalian 116034, China*

Yancheng Yu − *Jiangxi Chinese Medicine Science Center of DICP, CAS, Nanchang 330000, China*; orcid.org/0000-0002-9783-775X

Hongjie Fan − *Jiangxi Chinese Medicine Science Center of DICP, CAS, Nanchang 330000, China*

Han Zhou − *Key Lab of Separation Science for Analytical Chemistry, Dalian Institute of Chemical Physics, Chinese Academy of Sciences, Dalian 116034, China*

Tao Hou − *Key Lab of Separation Science for Analytical Chemistry, Dalian Institute of Chemical Physics, Chinese Academy of Sciences, Dalian 116034, China; Jiangxi Chinese Medicine Science Center of DICP, CAS, Nanchang 330000, China*

Yonglin Ge − *Jiangxi Chinese Medicine Science Center of DICP, CAS, Nanchang 330000, China*

Jixia Wang − *Key Lab of Separation Science for Analytical Chemistry, Dalian Institute of Chemical Physics, Chinese Academy of Sciences, Dalian 116034, China; Jiangxi Chinese Medicine Science Center of DICP, CAS, Nanchang 330000, China*

Zhimou Guo − *Key Lab of Separation Science for Analytical Chemistry, Dalian Institute of Chemical Physics, Chinese Academy of Sciences, Dalian 116034, China; Jiangxi Chinese Medicine Science Center of DICP, CAS, Nanchang 330000, China*; orcid.org/0000-0001-7129-186X

Yang Chen − *Key Lab of Separation Science for Analytical Chemistry, Dalian Institute of Chemical Physics, Chinese Academy of Sciences, Dalian 116034, China; Jiangxi Chinese Medicine Science Center of DICP, CAS, Nanchang 330000, China*

Complete contact information is available at: https://pubs.acs.org/10.1021/acsmedchemlett.2c00461

Author Contributions

†Lai Wei and Kaijing Xiang contributed equally to this work. Author contributions are the following: conceptualization, Yaopeng Zhao, Xinmiao Liang; chemistry: Lai Wei, Yonglin Ge; biology, Lai Wei, Kaijing Xiang, Hongjian Kang, Hongjie Fan, Tao Hou, Yang Chen; writings, Yancheng Yu, Han Zhou, Jixia Wang, Zhimou Guo. The manuscript was written through contributions of all authors. All authors have given approval to the final version of the manuscript.

Notes

The authors declare no competing financial interest.

■ ACKNOWLEDGMENTS

This work was supported by the innovation program of science and research from DICP, CAS (DICP ZZBS201803).

■ ABBREVIATIONS

GPCR, G protein-coupled receptor; hGPR35, human G protein-coupled receptor 35; BRET, bioluminescent resonance energy transfer; NLUC, nano-luciferase; DMR, dynamic mass redistribution; BODIPY, 4,4-difluoro-4-bora-3a,4a-diaza-s-indacene

■ REFERENCES

(1) O'Dowd, B. F.; Nguyen, T.; Marchese, A.; Cheng, R.; Lynch, K. R.; Heng, H. H. Q.; Kolakowski, L. F.; George, S. R. Discovery of three novel G-protein-coupled receptor genes. *Genomics* **1998**, *47*, 310−313.

(2) Baumgartner, R.; Casagrande, F. B.; Mikkelsen, R. B.; Berg, M.; Polyzos, K. A.; Forteza, M. J.; Arora, A.; Schwartz, T. W.; Hjorth, S. A.; Ketelhuth, D. F. J. Disruption of GPR35 Signaling in Bone Marrow-Derived Cells Does Not Influence Vascular Inflammation and Atherosclerosis in Hyperlipidemic Mice. *Metabolites* **2021**, *11*, 411.

(3) Boleij, A.; Fathi, P.; Dalton, W.; Park, B.; Wu, X.; Huso, D.; Allen, J.; Besharati, S.; Anders, R. A.; Housseau, F. G-protein coupled receptor 35 (GPR35) regulates the colonic epithelial cell response to enterotoxigenic Bacteroides fragilis. *Commun. Biol.* **2021**, *4*, 585.

(4) Quon, T.; Lin, L.-C.; Ganguly, A.; Tobin, A. B.; Milligan, G. Therapeutic Opportunities and Challenges in Targeting the Orphan G Protein-Coupled Receptor GPR35. *ACS Pharmacol Transl* **2020**, *3*, 801−812.

(5) Maravillas-Montero, J. L.; Burkhardt, A. M.; Hevezi, P. A.; Carnevale, C. D.; Smit, M. J.; Zlotnik, A. Cutting Edge: GPR35/CXCR8 Is the Receptor of the Mucosal Chemokine CXCL17. *J. Immunol* **2015**, *194*, 29−33.

(6) Park, S.-J.; Lee, S.-J.; Nam, S.-Y.; Im, D.-S. GPR35 mediates lodoxamide-induced migration inhibitory response but not CXCL17-induced migration stimulatory response in THP-1 cells; is GPR35 a receptor for CXCL17? *Br. J. Pharmacol.* **2018**, *175*, 154−161.

(7) Shore, D. M.; Reggio, P. H. The therapeutic potential of orphan GPCRs, GPR35 and GPR55. *Front Pharmacol* **2015**, *6*, DOI: 10.3389/fphar.2015.00069.

(8) Binti Mohd Amir, N. A. S.; Mackenzie, A. E.; Jenkins, L.; Boustani, K.; Hillier, M. C.; Tsuchiya, T.; Milligan, G.; Pease, J. E. Evidence for the Existence of a CXCL17 Receptor Distinct from GPR35. *J. Immunol* **2018**, *201*, 714−724.

(9) Thimm, D.; Funke, M.; Meyer, A.; Mueller, C. E. 6-Bromo-8-(4-H-3 methoxybenzamido)-4-oxo-4H-chromene-2-carboxylic Acid: A Powerful Tool for Studying Orphan G Protein-Coupled Receptor GPR35. *J. Med. Chem.* **2013**, *56*, 7084−7099.
(10) Loudet, A.; Burgess, K. BODIPY dyes and their derivatives: Syntheses and spectroscopic properties. *Chem. Rev.* **2007**, *107*, 4891−4932.
(11) Norager, N. G.; Jensen, C. B.; Rathje, M.; Andersen, J.; Madsen, K. L.; Kristensen, A. S.; Stromgaard, K. Development of Potent Fluorescent Polyamine Toxins and Application in Labeling of Ionotropic Glutamate Receptors in Hippocampal Neurons. *ACS Chem. Biol.* **2013**, *8*, 2033−2041.
(12) Wei, L.; Hou, T.; Li, J.; Zhang, X.; Zhou, H.; Wang, Z.; Cheng, J.; Xiang, K.; Wang, J.; Zhao, Y.; Liang, X. Structure-Activity Relationship Studies of Coumarin-like Diacid Derivatives as Human G Protein-Coupled Receptor-35 (hGPR35) Agonists and a Consequent New Design Principle. *J. Med. Chem.* **2021**, *64*, 2634−2647.
(13) Telegin, F. Y.; Marfin, Y. S. Polarity and Structure of BODIPYs: A Semiempirical and Chemoinformation Analysis. *Russ. J. Inorg. Chem.* **2022**, *67*, 362−374.
(14) Nano, A.; Ziessel, R.; Stachelek, P.; Harriman, A. Charge-Recombination Fluorescence from Push-Pull Electronic Systems Constructed around Amino-Substituted Styryl-BODIPY Dyes. *Chem.—Eur. J.* **2013**, *19*, 13528−13537.
(15) Petrushenko, K. B.; Petrushenko, I. K.; Petrova, O. V.; Sobenina, L. N.; Ushakov, I. A.; Trofimov, B. A. Environment-Responsive 8-CF3-BODIPY Dyes with Aniline Groups at the 3 Position: Synthesis, Optical Properties and RI-CC2 Calculations. *Asia J. Org. Chem.* **2017**, *6*, 852−861.
(16) Conroy, S.; Kindon, N. D.; Glenn, J.; Stoddart, L. A.; Lewis, R. J.; Hill, S. J.; Kellam, B.; Stocks, M. J. Synthesis and Evaluation of the First Fluorescent Antagonists of the Human P2Y(2) Receptor Based on AR-C118925. *J. Med. Chem.* **2018**, *61*, 3089−3113.
(17) Thakare, S. S.; Chakraborty, G.; Kothavale, S.; Mula, S.; Ray, A. K.; Sekar, N. Proton Induced Modulation of ICT and PET Processes in an Imidazo-phenanthroline Based BODIPY Fluorophores. *J. Fluoresc* **2017**, *27*, 2313−2322.
(18) Deng, H.; Hu, H.; Ling, S.; Ferrie, A. M.; Fang, Y. Discovery of Natural Phenols as G Protein-Coupled Receptor-35 (GPR35) Agonists. *ACS Med. Chem. Lett.* **2012**, *3*, 165−169.
(19) Deng, H.; Hu, H.; Fang, Y. Multiple tyrosine metabolites are GPR35 agonists. *Sci. Rep.* **2012**, *2*, 373.
(20) Hall, M. P.; Unch, J.; Binkowski, B. F.; Valley, M. P.; Butler, B. L.; Wood, M. G.; Otto, P.; Zimmerman, K.; Vidugiris, G.; Machleidt, T.; Robers, M. B.; Benink, H. A.; Eggers, C. T.; Slater, M. R.; Meisenheimer, P. L.; Klaubert, D. H.; Fan, F.; Encell, L. P.; Wood, K. V. Engineered luciferase reporter from a deep sea shrimp utilizing a novel imidazopyrazinone substrate. *ACS Chem. Biol.* **2012**, *7*, 1848−1857.
(21) Stoddart, L. A.; Johnstone, E. K. M.; Wheal, A. J.; Goulding, J.; Robers, M. B.; Machleidt, T.; Wood, K. V.; Hill, S. J.; Pfleger, K. D. G. Application of BRET to monitor ligand binding to GPCRs. *Nat. Methods* **2015**, *12*, 661−663.
(22) Yang, Y.; Lu, J. Y.-L.; Wu, X.; Summer, S.; Whoriskey, J.; Saris, C.; Reagan, J. D. G-Protein-Coupled Receptor 35 Is a Target of the Asthma Drugs Cromolyn Disodium and Nedocromil Sodium. *Pharmacology* **2010**, *86*, 1−5.
(23) Deng, H.; Hu, H.; He, M.; Hu, J.; Niu, W.; Ferrie, A. M.; Fang, Y. Discovery of 2-(4-Methylfuran-2(5H)-ylidene)malononitrile and Thieno 3,2-b thiophene-2-carboxylic Acid Derivatives as G Protein-Coupled Receptor 35 (GPR35) Agonists. *J. Med. Chem.* **2011**, *54*, 7385−7396.
(24) Hu, H.; Deng, H.; Fang, Y. Label-Free Phenotypic Profiling Identified D-Luciferin as a GPR35 Agonist. *PLoS One* **2012**, *7*, e34934.
(25) Zhao, P.; Sharir, H.; Kapur, A.; Cowan, A.; Geller, E. B.; Adler, M. W.; Seltzman, H. H.; Reggio, P. H.; Heynen-Genel, S.; Sauer, M.; Chung, T. D. Y.; Bai, Y.; Chen, W.; Caron, M. G.; Barak, L. S.; Abood, M. E. Targeting of the Orphan Receptor GPR35 by Pamoic Acid: A Potent Activator of Extracellular Signal-Regulated Kinase and beta-Arrestin2 with Antinociceptive Activity. *Mol. Pharmacol.* **2010**, *78*, 560−568.
(26) Wei, L.; Wang, J.; Zhang, X.; Wang, P.; Zhao, Y.; Li, J.; Hou, T.; Qu, L.; Shi, L.; Liang, X.; Fang, Y. Discovery of 2H-Chromen-2-one Derivatives as G Protein-Coupled Receptor-35 Agonists. *J. Med. Chem.* **2017**, *60*, 362−372.
(27) Wei, L.; Hou, T.; Lu, C.; Wang, J.; Zhang, X.; Fang, Y.; Zhao, Y.; Feng, J.; Li, J.; Qu, L.; Piao, H. L.; Liang, X. SAR Studies of N-[2-(1H-Tetrazol-5-yl)phenyl]benzamide Derivatives as Potent G Protein-Coupled Receptor-35 Agonists. *ACS Med. Chem. Lett.* **2018**, *9*, 422−427.
(28) Christiansen, E.; Hudson, B. D.; Hansen, A. H.; Milligan, G.; Ulven, T. Development and Characterization of a Potent Free Fatty Acid Receptor 1 (FFA1) Fluorescent Tracer. *J. Med. Chem.* **2016**, *59*, 4849−58.

https://doi.org/10.1021/acsmedchemlett.2c00461
ACS Med. Chem. Lett. 2023, 14, 411−416